Recent Trends in the Study of Compact Objects: Theory and Observation
ASI Conference Series, 2013, Vol. 8, pp 147–150
Edited by Santabrata Das, Anuj Nandi and Indranil Chattopadhyay

Study of jet properties around compact objects with the change in accretion disc parameters

Rajiv Kumar[1,2*], Indranil Chattopadhyay[1] and Samir Mandal[3]
[1]*ARIES, Manora Peak, Nainital-263002, India*
[2]*School of Studies in Physics & Astrophysics, Pt. Ravishankar Shukla University, Raipur-492010(CG), India*
[3]*IIST, Trivandrum, India.*

Abstract. We have investigated radiatively and thermally driven self-consistent bipolar outflows from shocked viscous accretion disc. We have found that radiations from the post-shock disc affects the subsonic part of the jets and mass outflow rate while pre-shock disc affects the only supersonic part of the jets.

Keywords : black hole physics – accretion, accretion discs – outflows – hydrodynamics

1. Introduction

Jets are a common feature of accreting black holes on all mass scales from AGNs to microquasars, but it can only originate from the accretion disc. Detailed observation of inner core of M87 showed that the jet originates from the inner part of the accretion disc (Junor et al. 1999). The connection between jet states and spectral states of the disc has been firmly established (Gallo et al. 2003; Fender et al. 2010) for microquasars, and is expected to be similar in AGNs too. Therefore, interaction of the jets and the radiation from the accretion disc should be studied. While Icke (1989) showed that the maximum terminal speed of a radiatively driven jet is $0.45c$ (c, speed of light), but Fukue et al. (2001) showed particle relativistic jet can be generated from luminous slim and ADAF disc. Chattopadhyay and Chakrabarti (2002); Chattopadhyay et al. (2004); Chattopadhyay (2005) on the other hand showed relativistic jets driven by radiations from a shocked accretion disc follows the observational correlation of the jet states and the spectral states of the accretion disc (Gallo et al. 2003). However, self-consistent thermally driven rotating jets from shocked accretion discs have been investigated by Chakrabarti (1999); Chattopadhyay and Das (2007); Das and Chattopadhyay (2008); Kumar and Chattopadhyay (2013); Kumar et al. (2013). In most studies of jet acceleration, the generation mechanism is ignored (Icke 1989; Fukue et

*email: rajiv.k@aries.res.in; indra@aries.res.in; samir@iist.ac.in

al. 2001; Chattopadhyay and Chakrabarti 2002), however presently, we study the generation (via shocks) and acceleration (via radiative and thermal driving) mechanism of the jets simultaneously with the accretion disc solutions, and therefore these jets are termed 'self-consistent'. In the section 2, we present equations and assumptions, in the last section solutions and discussion.

2. Fluid equations of motion and assumptions

We consider axisymmetric viscous accretion disc around equatorial plane in cylindrical co-ordinate and it is presented in detail in many literature (Kumar and Chattopadhyay 2013, and references therein). Here we consider the same methodology to compute the jet as described in Kumar and Chattopadhyay (2013) but with the deposition of radiative moments from the accretion disc onto the jet as shown by Chattopadhyay and Chakrabarti (2002); Chattopadhyay et al. (2004). We use geometrical units $2G = M = c = 1$, where M is mass of the black hole, G is gravitational constant. We are not presenting the accretion equations and solution methodology for brevity of space. Momentum balance equation of the jet in presence of radiation field and correct upto first order in velocity, is given by (Mihalas and Mihalas 1984; Chattopadhyay and Chakrabarti 2002)

$$v_j \frac{dv_j}{dr} + \frac{1}{\rho_j}\frac{dp_j}{dr} - \frac{\lambda_j^2}{x_j^3}\frac{dx_j}{dr} + \frac{1}{2(r_j-1)^2}\frac{dr_j}{dr} = \mathcal{F}_{r_j} - v_j(\mathcal{E}_{r_j} + \mathcal{P}_{r_j}) \tag{1}$$

here, $\mathcal{F}_{r_j} = \sigma_T F_{r_j}/m_e c, \mathcal{E}_{r_j} = \sigma_T E_{r_j}/m_e$, and $\mathcal{P}_{r_j} = \sigma_T P_{r_j}/m_e$, where, σ_T is the Thompson scattering cross-section, m_e is the electron mass, and F_{r_j}, E_{r_j}, P_{r_j} are radiative flux, radiative energy density and radiative pressure, respectively. The first term in r. h. s of Eq. (1) is the acceleration term, while negative terms are the radiative drag term. All the terms with the suffix 'j' represents jet quantities. The pre-shock radiation is assumed due to only the synchrotron emission. The synchrotron emissivity is due to the presence of stochastic magnetic field, where the magnetic pressure (p_m) is in partial equipartition with the gas pressure (p_g), i.e. $p_m = \frac{B^2}{8\pi} = \beta p_g$; where, $0 \le \beta \le 1$. The analytical expression for synchrotron emissivity is given by Shapiro and Teukolsky (1983), and the resulting intensity is,

$$I_{ps} = I_{syn} = \frac{16}{3}\frac{e^2}{c}\left(\frac{eB}{m_e c}\right)^2 \Theta^2 n_e \left(\frac{hr_g}{sec\theta_{ps}}\right) \text{ erg cm}^{-2}\text{s}^{-1} \tag{2}$$

where, Θ, n_e, h and θ_{ps} are the pre-shock local dimensionless temperature $k_b T/(m_e c^2)$, electron number density, disc half height and angle from the axis of symmetry to the pre-shock disc surface, respectively. The dependence of I_{ps} on disc radius is through flow variable like T and n_e. This is the dominant emission from the pre-shock disc. The radiative intensity from the post shock disc is $I_s = \ell_s/A_s$, where ℓ_s is the post-shock luminosity in units of Eddington luminosity, and A_s is the total surface area of the post-shock disc. The accretion solutions are parametrized by the grand specific energy E, the specific angular momentum on the horizon λ_0, and the viscosity

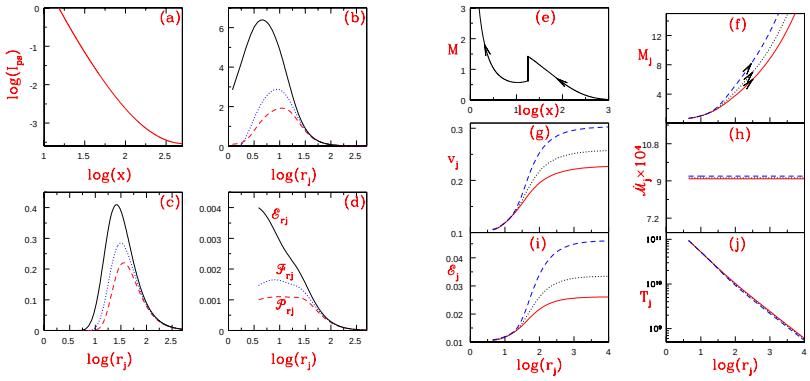

Figure 1. (a) Normalized intensity of pre-shock synchrotron radiation I_{ps} with $log(x)$, (b) Radiative Moments due to the post-shock disc $\mathcal{E}_{r_j s}/\mathcal{K}_0$ (solid), $\mathcal{F}_{r_j s}/\mathcal{K}_0$ (dotted) and $\mathcal{P}_{r_j s}/\mathcal{K}_0$ (dashed), are plotted with $log(r_j)$, and (c) $\mathcal{E}_{r_j ps}/\mathcal{J}_0$ (solid), $\mathcal{F}_{r_j ps}/\mathcal{J}_0$ (dotted) and $\mathcal{P}_{r_j ps}/\mathcal{J}_0$ (dashed), the radiative moments from the pre-shock disc are plotted. (d) Total radiative moments from the entire disc. We plot (e) M and (f) M_j with radial distance x and jet streamline r_j in log scale. Arrows show flow directions. And the velocity v_j (g), entropy accretion rate $\dot{\mathcal{M}}_j$ (h), specific energy $\mathcal{E}_j$ (i), and the temperature T_j (j) of the jet are plotted. Accretion flow parameters are $E = 3.3 \times 10^{-3}$, $\lambda_0 = 1.353$, $\alpha = 0.1$. The plots are for constant $\ell_s = 0.1$.

parameter α. In Figs. 1a-d, all the plots are generated for a disc characterized by $(E, \lambda_0, \alpha) = (3.5 \times 10^{-3}, 1.5435, 0.02)$, the shock location is at $x_s = 15.18$. The moments of the radiation field above the accretion disc was calculated before (Chattopadhyay and Chakrabarti 2002; Chattopadhyay et al. 2004; Chattopadhyay 2005), and for the above mentioned approximations, they are given by, $\mathcal{E}_{r_j} = \frac{\sigma_T}{mc}\left(\int I d\Omega\right) = \mathcal{K}_0\mathcal{E}_s(r_j, x) + \mathcal{J}_0\mathcal{E}_{ps}(r_j, x)$, $\mathcal{F}_{r_j} = \frac{\sigma_T}{mc}\left(\int I_{\hat{r_j}} d\Omega\right) = \mathcal{K}_0\mathcal{F}_s(r_j, x) + \mathcal{J}_0\mathcal{F}_{ps}(r_j, x)$, and $\mathcal{P}_{r_j} = \frac{\sigma_T}{mc}\left(\int I \hat{r_j}\hat{r_j} d\Omega\right) = \mathcal{K}_0\mathcal{P}_s(r_j, x) + \mathcal{J}_0\mathcal{P}_{ps}(r_j, x)$ where, $\mathcal{K}_0 = \frac{1.3\times10^{38}\ell_s\sigma_T}{2\pi c m_p A_s G M_\odot}$, $\mathcal{J}_0 = \frac{2.93\times10^{34}e^4\mu^2\beta\sigma_T\dot{m}^2}{3\pi m_e^4 c^2 sec\theta_{ps}\gamma^{5/2}G^2M_\odot^2}$, $\dot{m}$ is the accretion rate in units of Eddington accretion rate, σ_T is Thomson scattering cross section, μ is mean molecular weight of the plasma, m_p is the proton mass, m_e is the electron mass and $M_\odot$ is the solar mass. The pre-shock radiation depends on the product $\beta\dot{m}^2$.

3. Accretion-ejection solutions and discussion

In Fig. 1a, we plot the pre-shock intensity I_{ps} due to synchrotron cooling as a function of $log(x)$. In Fig. 1b, we plot post shock radiative moments like $\mathcal{E}_{r_j s}/\mathcal{K}_0$ (solid), $\mathcal{F}_{r_j s}/\mathcal{K}_0$ (dotted) and $\mathcal{P}_{r_j s}/\mathcal{K}_0$ (dashed). In Fig. 1c, we plot pre-shock radiative moments $\mathcal{E}_{r_j ps}/\mathcal{J}_0$ (solid), $\mathcal{F}_{r_j ps}/\mathcal{J}_0$ (dotted) and $\mathcal{P}_{r_j ps}/\mathcal{J}_0$ (dashed). In Fig. 1d, we plot the combined radiative moments $\mathcal{E}_{r_j}$ (solid), $\mathcal{F}_{r_j}$ (dotted), and $\mathcal{P}_{r_j}$ (dashed), which shows that the moments peaks at two positions above the disc, raising possibility of multistage acceleration. Moreover, the pre-shock radiation is blocked by the post-shock puffed up inner disc (Fig. 1c), so the pre-shock radiation interacts with the

supersonic part of the jet. On closer inspection the net radiative acceleration term $\mathcal{F}_{r_j} - v_j(\mathcal{E}_{r_j} + \mathcal{P}_{r_j})$, show that it is dependent on v_j, and above certain v_j this term may even be negative. However, at larger distances away from the disc $\mathcal{E}_{r_j} \approx \mathcal{F}_{r_j} \approx \mathcal{P}_{r_j}$ (Fig. 1b-d), we get the highest v_j possible. If the acceleration is closer to the base, then it would affect the subsonic part of the jet, and would decrease the location of the jet sonic point, and also increase the mass outflow rate $R_{\dot{m}}$, which would, in turn, decrease the accretion shock location. However, if there is significant acceleration in the supersonic part due to the pre-shock radiation then only the velocity of the jet will be affected without consequent increase in inertia of the jet. Since pre and post shock radiation maximizes at different locations (Figs. 1b, c), so a multistage acceleration may produce large terminal speed. Fig. 1e-j, we illustrate the effect of radiation from pre-shock disc (ℓ_{ps}) on the jet flow variables and keeping $\ell_s = 0.1$ constant. In Fig. 1e we plot accretion Mach number ($M = v/a$) and Fig. 1f, the jet Mach number(M_j) is plotted. We also plot the velocity v_j (Fig. 1g), $\dot{\mathcal{M}}_j$ (Fig.1h), specific energy $\mathcal{E}_j$ (Fig. 1i), and the temperature of T_j (Fig. 1j) of the jet. Accretion parameters are $E = 3.3 \times 10^{-3}$, $\lambda_0 = 1.353$, $\alpha = 0.1$ (Figs. 1e-j). Each curve corresponds to $\dot{m} = 0.1$ (solid), 0.2 (dotted), 0.4 (dashed) and $\beta = 1$. Here jet base, shock location, jet sonic point and mass outflow rate are unaffected by the change in pre-shock radiation. Supersonic part of the jet is very much affected (Figs. 1e-j).

We can conclude that radiations from the pre and post shock disc participate in multistage acceleration of the jets. Since radiation from the post-shock disc affect the jet base and jet critical point, it is effective in acceleration at the initiation, but acceleration in the supersonic part by the radiations from pre-shock disc generates jets with really high terminal speed.

References

Chakrabarti S. K., 1999, A&A, 351, 185
Chattopadhyay I., Chakrabarti S. K., 2002, MNRAS, 333, 454.
Chattopadhyay I., Das S., Chakrabarti S. K., 2004, MNRAS, 348, 846.
Chattopadhyay I., 2005, MNRAS, 356, 145
Chattopadhyay I., Das S., 2007, New A, 12, 454
Das S., Chattopadhyay I., 2008, New A, 13, 549.
Fender R. P., Gallo E., Russell D., 2010, MNRAS, 406, 1425.
Fukue J., Tojyo M., Hirai Y., 2001, PASJ, 53, 555
Gallo E., Fender R. P., Pooley G., 2003, MNRAS, 344, 60
Icke V., 1989, A&A, 216, 294
Junor W., Biretta J. A., Livio M., 1999, Nature, 401, 891
Kumar R., et al., 2013, MNRAS, doi 10.1093/mnras/stt1781
Kumar R., Chattopadhyay I., 2013, MNRAS, 430, 386
Mihalas D., Mihalas B. W., 1984, Foundations of Radiation Hydrodynamics. Oxford Univ. Press, Oxford.
Shapiro S. L., Teukolsky S. A., 1983, Black Holes, White Dwarfs and Neutron Stars, Physics of Compact Objects. Wiley-Interscience, New York.